INTERNATIONAL JOURNAL OF SYSTEMATIC AND EVOLUTIONARY MICROBIOLOGY

TAXONOMIC DESCRIPTION

Benndorf *et al.*, *Int. J. Syst. Evol. Microbiol.* 2020;70:5255–5262

DOI 10.1099/ijsem.0.004403

MICROBIOLOGY SOCIETY

OPEN ACCESS

Actinomadura rubteroloni sp. nov. and *Actinomadura macrotermitis* sp. nov., isolated from the gut of the fungus growing-termite *Macrotermes natalensis*

René Benndorf[1], Karin Martin[2,*], Michelle Küfner[1], Z. Wilhelm de Beer[3], John Vollmers[4], Anne-Kristin Kaster[4] and Christine Beemelmanns[1,*]

Abstract

The taxonomic positions of two novel aerobic, Gram-positive actinobacteria, designated strains RB29^T and RB68^T, were determined using a polyphasic approach. Based on 16S rRNA gene sequence analysis, the closest phylogenetic neighbours of RB29^T were identified as *Actinomadura rayongensis* DSM 102126^T (99.2% similarity) and *Actinomadura atramentaria* DSM 43919^T (98.7%), and for strain RB68^T was *Actinomadura hibisca* DSM 44148^T (98.3%). Digital DNA–DNA hybridization (dDDH) between RB29^T and its closest phylogenetic neighbours, *A. rayongensis* DSM 102126^T and *A. atramentaria* DSM 43919^T, resulted in similarity values of 53.2% (50.6–55.9%) and 26.4% (24.1–28.9%), respectively. Additionally, the average nucleotide identity (ANI) was 93.2% (94.0%) for *A. rayongensis* DSM 102126^T and 82.3% (78.9%) for *A. atramentaria* DSM 43919^T. dDDH analysis between strain RB68^T and *A. hibisca* DSM 44148^T gave a similarity value of 24.5% (22.2–27.0%). Both strains, RB29^T and RB68^T, revealed morphological characteristics and chemotaxonomic features typical for the genus *Actinomadura*, such as the presence of *meso*-diaminopimelic acid in the cell wall, galactose and glucose as major sugar components within whole-cell hydrolysates and the absence of mycolic acids. The major phospholipids were diphosphatidylglycerol, phosphatidylglycerol, phosphatidylinositol and phosphatidylinositol mannoside. Predominant menaquinones were MK-9(H_6) and MK-9(H_8) for RB29^T and MK-9(H_4) and MK-9(H_6) for RB68^T. The main fatty acids were identified as 10-methyloctadecanoic acid (10-methyl $C_{18:0}$), 14-methylpentadecanoic acid (iso-$C_{16:0}$), hexadecanoic acid ($C_{16:0}$) and *cis*-9-octadecanoic acid ($C_{18:1}$ ω9*c*). Here, we propose two novel species of the genus *Actinomadura*: *Actinomadura rubteroloni* sp. nov. with the type strain RB29^T (=CCUG 72668^T=NRRL B-65537^T) and *Actinomadura macrotermitis* sp. nov. with the type strain RB68^T (=CCUG 72669^T=NRRL B-65538^T).

INTRODUCTION

Lechevalier and Lechevalier were the first to describe the genus *Actinomadura* based on the type species *Actinomadura madurae* [1, 2]. *Actinomadura* belongs to the family *Thermomonosporaceae* together with the genera *Thermomonospora*, *Spirillospora*, *Actinocorallia* and *Actinoallomurus* [3, 4]. Members of the genus *Actinomadura* have a characteristic non-fragmenting, extensively branched substrate mycelium and moderate or absent aerial mycelia, which differentiate when formed into chains of spores. Species of *Actinomadura* are described as aerobic, Gram-positive, non-motile organisms. Characteristic chemotaxonomic markers of *Actinomadura* are *meso*-diaminopimelic acid (A_2pm) as the diagnostic diaminoacid of the cell wall, and galactose, glucose, madurose, mannose and ribose as major components in cell-wall hydrolysates. Cell membranes

Author affiliations: [1]Chemical Biology of Microbe–Host Interactions, Leibniz Institute for Natural Product Research and Infection Biology e. V., Hans-Knöll-Institute, Beutenbergstraße 11a, 07745 Jena, Germany; [2]Bio Pilot Plant, Leibniz Institute for Natural Product Research and Infection Biology e. V., Hans-Knöll-Institute, Beutenbergstraße 11a, 07745 Jena, Germany; [3]Department of Biochemistry, Genetics and Microbiology, Forestry and Agriculture Biotechnology Institute, University of Pretoria, Pretoria, South Africa; [4]Institute for Biological Interfaces 5, Karlsruhe Institute of Technology, Hermann-von-Helmholtz-Platz 1, 76344 Eggenstein-Leopoldshafen, Germany.

***Correspondence:** Christine Beemelmanns, christine.beemelmanns@leibniz-hki.de; Karin Martin, Karin.Martin@leibniz-hki.de

Keywords: *Actinomadura*; *Macrotermes natalensis*; new natural products; termite gut.

Abbreviations: ANI, average nucleotide identity; ANI, average nucleotide identity; A2pm, diaminopimelic acid; A2pm, diaminopimelic acid; dDDH, digital DNA-DNA hybridization; dDDH, digital DNA–DNA hybridization.

The GenBank/EMBL/DDBJ accession numbers for the 16S rRNA gene sequences of strain RB29^T and RB68^T are KY312019.2 and MH044510.2, respectively. The Whole Genome Shotgun projects have been deposited at DDBJ/ENA/GenBank under INSDC accession numbers MTBP00000000 and WEGH00000000 respectively. The versions described in this paper are versions MTBP00000000.1 and WEGH00000000.1. The raw sequencing data have been deposited under accession numbers SRR11565158 and SRR11566452, respectively.

Seven supplementary tables and nine supplementary figures are available with the online version of this article.

consist dominantly of phosphatidylinositol and diphosphatylglycerol, and habour minor amounts of phosphatidylinositol and phosphatidylinositol mannoside [1, 5]. Predominant menaquinones are MK-9(H_4), MK-9(H_6) and MK-9(H_8) [6, 7]. The fatty acid profiles of *Actinomadura* species are found to be mostly complex mixtures of hexadecanoic ($C_{16:0}$), 14-methylpentadecanoic (iso-$C_{16:0}$) and 10-methyloctadecanoic acid [4]. *Actinomadura* species have been isolated from diverse habitats such as soil [5–8], marine sources [9], plant tissues [10, 11] and bee hives [12], and are a known source of diverse bioactive secondary metabolites. Over the last three decades, different bioactive secondary metabolites have been reported, including polyether antibiotic [13], anthracycline [14], polyketide [15] and β-carboline [16].

ISOLATION AND ECOLOGY

Fungus-growing termite workers of *Macrotermes natalensis* were collected from two colonies, Mn160 (25° 44′ 34.7″ S 28° 15′ 38.7″ E) and Mn162 (24° 40′ 30.5″ S 28° 47′ 50.4″ E) in South Africa in February 2015 and isolation procedures have been described by Benndorf *et al.* [17]. We focused on the isolation of actinobacteria present within the termite gut and capable of living on cellulose or chitin as a sole carbon source as these bacterial isolates are likely to be adapted to living in a lignin- and cellulose-rich environment. Actinobacteria strains RB29^T and RB68^T showing distinct morphotypes appeared on chitin agar supplemented with cycloheximide (0.05 g l^{-1}) [18, 19] after aerobic incubation at 30 °C for 21 days [17]. Bacterial colonies were subcultured on yeast extract-malt extract agar (ISP2) [20] until clean isolates were obtained. Strains RB29^T (alias 5-2) and RB68^T were maintained on ISP2 at 30 °C and as glycerol suspensions (25%, v/v) at −80 °C.

16S rRNA PHYLOGENY

For phylogenetic analysis, 16S rRNA gene sequences were obtained from both strains (RB29^T and RB68^T) by PCR amplification [17] and additionally extracted from genomic data (*vide infra* Genomic Features) using Artemis [21]. BLAST analysis was performed using the NCBI database and 16S rRNA gene sequences of nearly all published *Actinomadura* reference strains downloaded from the LPSN database [22]. Pairwise sequence similarities were calculated using the method recommended by Meier-Kolthoff [23] on the GGDC web server available at http://ggdc.dsmz.de/ (Tables S1 and S2, available in the online version of this article). Sequences were aligned with the SINA sequence alignment service [24]. Phylogenetic trees were reconstructed with the neighbour-joining [25] and maximum-likelihood algorithms [26] in MEGA software (version 7.0.26) [27]. The evolutionary distance model of Tamura and Nei [28] was used to generate evolutionary distance matrices for the maximum-likelihood and neighbour-joining algorithms with deletion of complete gaps and missing data. For the maximum-likelihood algorithm, the discrete gamma distribution was used (+*G*) and the rate variation model allowing for some sites to be evolutionarily invariable (+*I*). For the neighbour-joining algorithm, rate variation among sites was modulated with a gamma distribution (+*G*). The confidence values of nodes were evaluated by bootstrap analysis based on 1000 re-samplings [29].

The results of our phylogenetic analysis can be summarized as follows. First, 16S rRNA gene sequence comparisons showed that strain RB29^T shared highest similarity with *Actinomadura rayongensis* DSM 102126^T (RY35-68^T) (99.2%) and *Actinomadura atramentaria* DSM 43919^T (98.7%). In contrast, strain RB68^T shared highest 16S rRNA gene sequence similarity with *Actinomadura hibisca* DSM 44148^T (ISMNU 22165^T=HKI14) (98.3%), *Actinomadura gamaensis* DSM 100815^T (NEAU-Gz5^T) (98.1%), *Actinomadura namibiensis* DSM 44197^T (98.0%) and *Actinomadura montaniterrea* CYP1-1B^T (98.0%). Lower levels of 16S rRNA gene sequence similarity (<98.0%) were found with the type strains of all other *Actinomadura* species (Tables S1 and S2).

Phylogenetic analysis based on maximum-likelihood and neighbour-joining trees revealed that strain RB29^T formed a cluster together with *A. rayongensis* DSM 102126^T, *A. atramentaria* DSM 43919^T and *A. flavalba* DSM 45200^T. Strain RB68^T formed a cluster with *A. hibisca* DSM 44148^T, *A. kijaniata* DSM 43764^T and *A. namibiensis* DSM 44197^T (Figs 1 and 2). These findings are supported by bootstrap values of 70% for RB29^T and *A. rayongensis* DSM 102126^T (=RY35-68^T) and 57% for RB68^T and *A. hibisca* DSM 44148^T (Figs 1 and 2).

GENOME FEATURES

Extraction of genomic DNA, PCR amplification/sequencing of the 16S rRNA gene and genome sequencing of strains RB29^T and RB68^T have been described previously [17, 30] and genome data have been deposited at NCBI under NZ_MTBP00000000.1 [RB29^T (alias 5-2)] and NZ_WEGH00000000.1 (RB68^T). Additionally, the genome of *A. rayongensis* DSM102126^T was sequenced (Genewiz) and genome data were deposited at NCBI (NZ_WUTW00000000.1, Table S4). The genomic DNA G+C content was determined from whole genome sequence data of strains RB29^T and RB68^T [31–33]. Digital DNA–DNA hybridization (dDDH) analysis was performed using the GGDC web service at http://ggdc.dsmz.de [32] and compared with other available published genomes of their corresponding genus. Additionally, average nucleotide identity (ANI) was calculated using the web services available at JSpeciesWS (http://jspecies.ribohost.com/jspeciesws) and EZBiocloud (https://www.ezbiocloud.net/tools/ani) (Tables S3 and S4) [34–36].

The results of the genomic analyses can be summarized as follows. First, whole genome sequences of strains RB29^T and RB68^T and of type strains of phylogenetically related *Actinomadura* species were used to construct a phylogenetic tree using the TYGS server (http://tygs.dsmz.de) [37]. The topology of the whole-genome sequence tree was similar to that obtained from 16S rRNA gene sequences (Figs 1 and 2).

We then determined the dDDH values (average and confidence intervals in parentheses) between strain RB29^T and

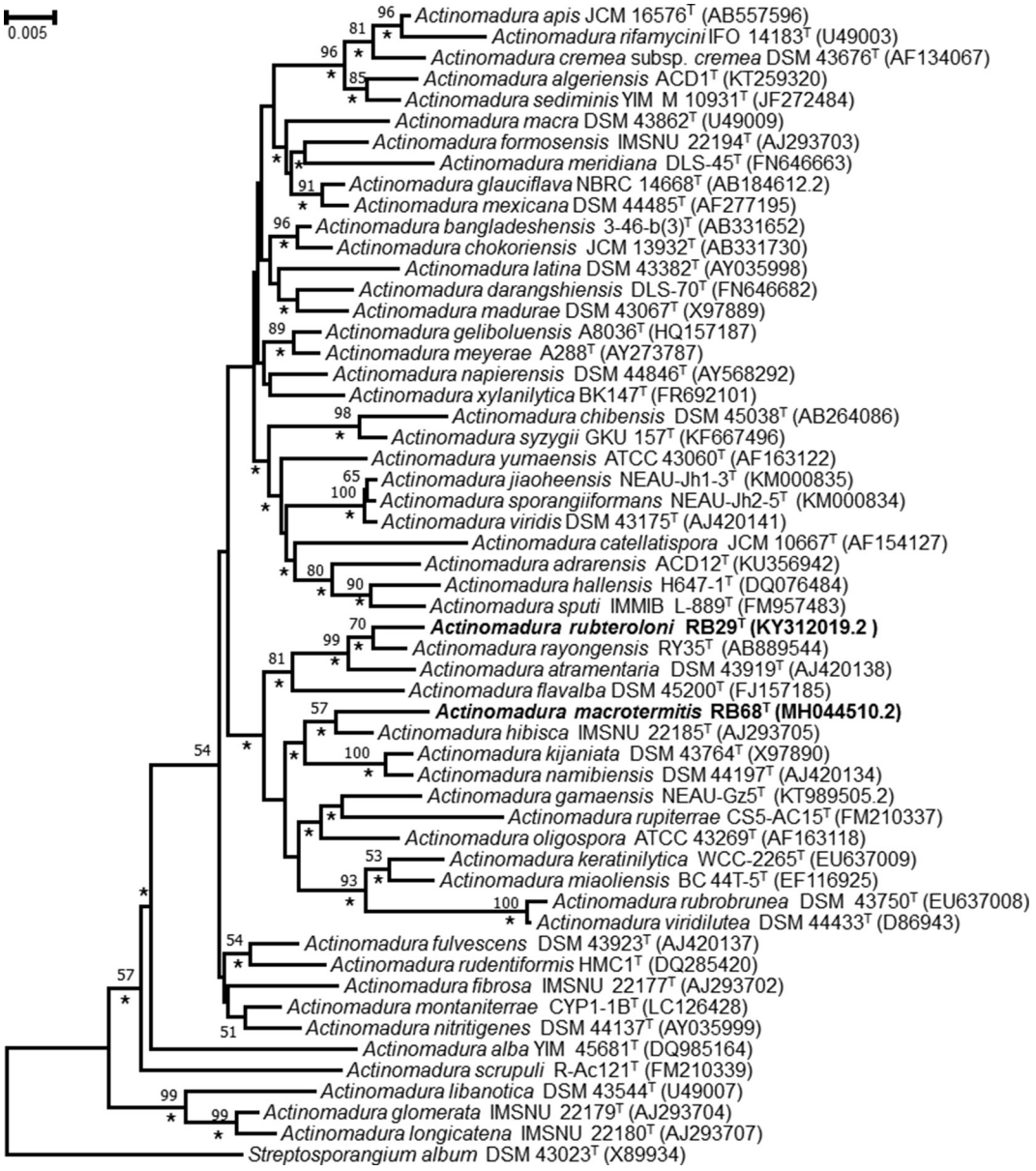

Fig. 1. Neighbour-joining tree based on almost-complete 16S rRNA gene sequences showing the relationships between strains RB29^T and RB68^T and species of the genus *Actinomadura*. *Streptosporangium album* DSM 43023^T was used as an outgroup. Asterisks indicate branches that were also recovered in the maximum-likelihood tree. Only bootstrap values above 50% (percentages of 1000 replications) are shown. Bar, 0.005 substitutions per nucleotide position.

its closest relatives *A. rayongensis* DSM 102126^T as 53.2% (50.6–55.9%) and *A. atramentaria* DSM 43919^T as 26.4% (24.1–28.9%). ANI values between strain RB29^T and *A. rayongensis* DSM 102126^T and *A. atramentaria* DSM 43919^T were 93.2% (94.0%) and 82.3% (78.9%), respectively. Overall, all calculated values were below the recommended threshold for the definition of a novel species [38]. Thus, we concluded at this step that strain RB29^T represents a novel bacterial species.

The dDDH value between strain RB68^T and its closest relative *A. hibisca* DSM 44148^T was determined as 24.5% (22.2–27.0%) (Table S3), below the threshold value of 70% for the delineation of bacterial species, indicating that RB68^T also represents a novel bacterial species.

Finally, the GC contents of strains RB29^T and RB68^T were calculated to be 73.1 mol% for both genomes (Table 1).

CHEMOTAXONOMY

For chemotaxonomic analyses, freeze dried biomass was obtained from cultures grown in ISP2 broth for 3 days at 28 °C on a rotary shaker at 180 r.p.m. The diagnostic diamino acid of the cell wall was determined in whole-cell hydrolysates

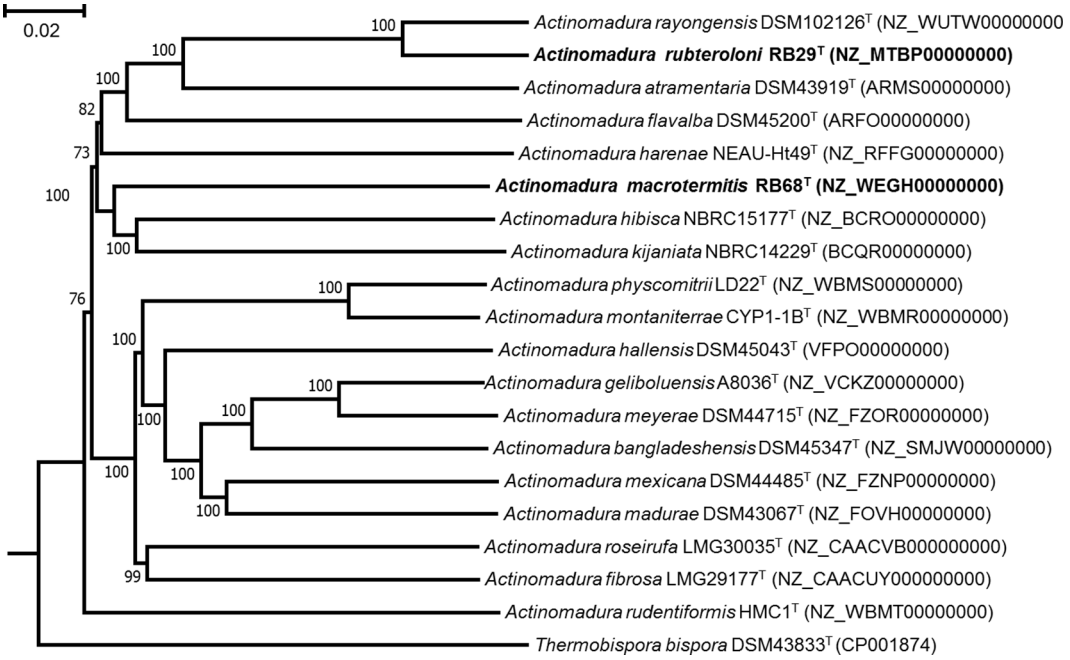

Fig. 2. Whole-genome sequence tree generated with TYGS for strains RB29^T and RB68^T and closely related *Actinomadura* strains. FastME used GBDP distances calculated from genome sequences. Branch lengths are scaled in terms of GBDP distance formula d5; numbers above branches are GBDP pseudo-bootstrap support values from 100 replications. The tree was processed with MEGA. *Thermobispora bispora* DSM 43833^T (CP001874) was used as an outgroup. Bar, 0.02 substitutions per nucleotide position.

by paper chromatography according to Hasegawa *et al.* [39]. Whole-cell sugars were examined according to Schumann [40]. The occurrence of mycolic acids was determined by TLC as described by Minnikin *et al.* [41]. Respiratory quinones were extracted and separated as described by Collins *et al.* [42] and subsequently analyzed as described by Wink *et al.* [43]. Polar lipids were extracted using the method described by Minnikin *et al.* [44] and identified by two-dimensional TLC as described by Collins and Jones (Figures S8 and S9) [45]. Extraction and analysis of fatty acids was performed by the DSMZ Identification service according to standard methods [46].

In summary, we found that whole-organism hydrolysates of strains RB29^T and RB68^T contained *meso*-A_2pm as the diagnostic diamino acid of the peptidoglycan, and carbohydrates composed of galactose, glucose, mannose and trace amounts of madurose (3-*O*-methyl-D-galactose, wall chemotype III *sensu*, Lechevalier *et al.*) [1], which are typical major carbohydrates found in members of the genus *Actinomadura*. Mycolic acids were not detected in the hydrolysates.

The menaquinone profile of strain RB29^T consisted of the predominant menaquinone MK-9(H_6) (75%), MK-9(H_8) (13%) and minor amounts of MK-10 (7%) and MK-9(H_4) (5%). The closest neighbour *A. rayongensis* DSM 102126^T exhibited a similar menaquinone ratio with MK-9(H_6) (71%), MK-9(H_8) (15%), MK-10 (7%) and MK-9(H_4) (7%), while *A. atramentaria* DSM 43919^T revealed a different profile of MK-9(H_6) (66%), MK-9(H_8) (16%), MK-9(H_4) (12%) and MK-10 (6%).

In contrast, strain RB68^T had a different menaquinone profile with major amounts of MK-9(H_4) (58%), MK-9(H_6) (30%) and minor amounts of MK-9(H_2) (6%) and MK-8 (6%). Here, the closest relative *A. hibisca* DSM 44148^T contained MK-9(H_6) (59%), MK-9(H_4) (25%), MK-9(H_8) (12%) and MK-10 (5%) and was thus different in its overall profile.

The major phospholipids found in strains RB29^T and RB68^T were diphosphatidylglycerol, phosphatidylinositol, phosphatidylinositol mannoside and phosphatidylglycerol, all of which are commonly found in most *Actinomadura* species (Table S7, Figs S8 and S9). RB29^T additionally contained two unidentified phospholipids, two lipids and a glycolipid.

The fatty acid profile of strain RB29^T (Table S7) was composed of the major fatty acids $C_{18:0}$ 10-methyl (22%), iso-$C_{16:0}$ (18.4%), $C_{17:0}$ 10-methyl (8.8%), $C_{16:0}$ (8.4%) and $C_{18:1}\omega9c$ (7.0%), and minor amounts of iso-$C_{18:0}$ (4.8%), iso-$C_{16:0}$ 2-OH (4.5%), $C_{18:0}$ (3.5%), $C_{16:1}\omega9c$ (2.8%), $C_{16:0}$ 2-OH (2.8%), $C_{16:0}$ 10-methyl (2.8%), $C_{19:0}$ cyclo C11–12 (2.6%), $C_{17:1}\omega9c$ (2.3%) and $C_{15:0}$ (2.0%).

In contrast, the closest related species *A. rayongensis* DSM 102126^T revealed a different fatty acid composition with the following major differences: $C_{16:0}$ (8.4% in RB29^T and 23.6% in *A. rayongensis* DSM 102126^T), $C_{17:0}$ 10-methyl (8.8% and 2.6%),

Table 1. Characteristic properties of strains RB29^T and RB68^T and related species

Strains: 1, RB29^T; 2, *A. rayongensis* DSM 102126^T; 3, *A. atramentaria* DSM 43919^T; 4, RB68^T; 5, *A. hibisca* DSM 44148^T. All data were acquired in this study. NT, Not tested. Utilization tests were analyzed as follows; +, grows like positive control (basal medium with glucose); (+), better than negative control but not like positive control; –, not better than negative control (basal medium with water). All strains were positive for utilization of D-glucose and negative for utilization of D-arabinose, D-xylose, D-mannitol, raffinose and cellulose

Characteristic	1	2	3	4	5
DNA G+C content (mol%)	73.1	73.1	73.7	73.1	72.4
Chemotaxonomic					
Major menaquinone	MK-9(H_6)	MK-9(H_6)	MK-9(H_6)	MK-9(H_4)	MK-9(H_6)
Major fatty acids (%)	$C_{18:0}$ 10-methyl (22), iso-$C_{16:0}$ (18.4)	$C_{16:0}$ (23.6), $C_{18:1}\omega9c$ (22.2)	$C_{18:0}$ 10-methyl (24.3), $C_{16:0}$ (18.2)	$C_{16:0}$ (30.7), $C_{18:1}\omega9c$ (19.7)	$C_{16:0}$ (15.7), $C_{18:1}\omega9c$ (14.5)
Diaminopimelic acid	*meso*-A_2pm	*meso*-A_2pm	*meso*-A_2pm	*meso*-A_2pm	*meso*-A_2pm
Mycolic acid	–	–	–	–	–
Physiological					
Growth temperature (°C)	20–37	20–45	15–42	15–37	18–40
Temperature optimum (°C)	25–30	30	30	25–30	30
pH tolerance range	5–7	5–8	5–8	6–8	6–8
Optimum pH	6–7	6–7	6–7	7	7
NaCl tolerance (%, w/v)	0–4	0–3	0–4	0–4	0–4
Optimum NaCl (%, w/v)	0–1	0–1	0–1	0–1	0–1
Carbon source					
Sucrose	–	–	–	–	(+)
Inositol	–	–	–	(+)	+
D-Fructose	–	–	–	(+)	(+)
L-Rhamnose	–	–	+	–	–

$C_{18:0}$ 10-methyl (22% and 14.1%), $C_{18:1}\omega9c$ (7.0% and 22.2%) and iso-$C_{16:0}$ (18.4% and 7.3%).

Analysis of strain RB68^T resulted in a different fatty acid profile with $C_{16:0}$ (30.7%), $C_{18:1}\omega9c$ (19.7%), $C_{18:0}$ 10-methyl (10%) and only minor amounts of $C_{16:1}\omega9c$ (9.7%), iso-$C_{16:0}$ (8.4%), $C_{14:0}$ (5%) and iso-$C_{18:0}$ (1.6%). The closest relative of RB68^T, *A. hibisca* DSM 44148^T, could be differentiated based on a more diverse profile consisting of $C_{16:0}$ (15.7%), $C_{18:1}\omega9c$ (14.5%), $C_{17:0}$ (13.9%) and $C_{17:1}\omega9c$ (10.6%). The latter two fatty acids were missing from strain RB68^T. Additionally, *A. hibisca* DSM 44148^T contained minor amounts of $C_{15:0}$ (8.1%), $C_{18:0}$ 10-methyl (6.9%), iso-$C_{16:0}$ (6.2%), $C_{16:1}\omega9c$ (5.2%), $C_{17:0}$ 10-methyl (4.5%), $C_{18:0}$ (3.5%) and $C_{14:0}$ (2.2%).

Overall, the fatty acid profiles clearly differentiate both new isolates from their closest relatives (Table 1).

PHYSIOLOGY

Morphological characteristics of the strains were determined on cultures grown for 5–14 days on ISP2 agar at 30 °C using a light microscope (Imager M2; Zeiss) and a field emission scanning electron microscope. Scanning electron microscopy was performed as described by Groth *et al.* [47]. Growth characteristics were determined on various ISP media for up to 18 days according to Shirling and Gottlieb [20] and similar to the approach described by Wink *et al.* [8]. Colony colour was determined using Baumanns Farbatlas 1 (Paul Baumann/Aue). Carbohydrate utilization was determined by using ISP9 (carbon utilization medium) supplemented with 1% of the sole carbon source. Melanoid pigment production was examined on peptone-yeast extract iron agar (ISP6), tyrosine agar (ISP7) and Suter medium [48] with and without tyrosine (1 g l^{-1}). Tolerance to NaCl was tested on ISP2 agar at concentrations of 1–15%. The pH tolerance (pH range 4–10) was tested in ISP2 broth using the buffer system described by Xu *et al.* [49], and temperature tolerance (4, 20, 28, 30, 37, 40, 45 and 60 °C) was tested on ISP2 agar.

The following morphological and phenotypic characteristics were documented for strains RB29^T and RB68^T, respectively (Table 1). RB29^T was capable of growing on all media tested, tolerated a pH range of 5.0–7.0 (optimal pH 7.0) and NaCl concentration of 0–4% (w/v) with optimal growth between 0 and 1% NaCl (Table 1). Note that strain

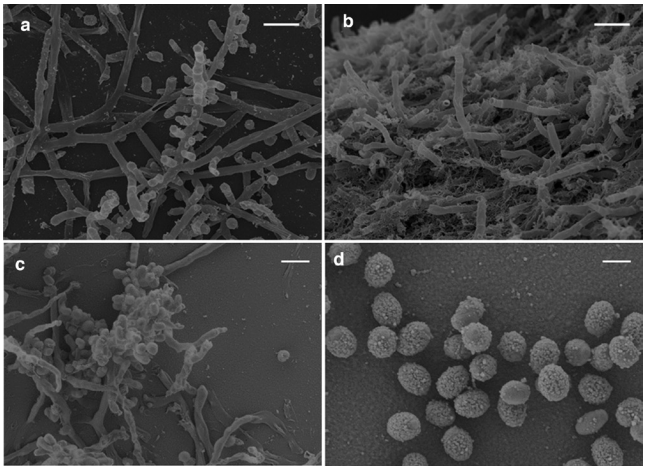

Fig. 3. Scanning electron micrographs of cells of strain RB29^T (a and c, bar 2 µm) and strain RB68^T (b, bar 2 µm and d, bar 1 µm) cultivated at 28 °C on ISP2 agar for 14 days.

RB29^T tolerated only growth temperatures of up to 37 °C, while *A. rayongensis* DSM 102126 grew even at a temperature of 45 °C. Substrate mycelium was pale (ISP1, ISP4), pale brownish (ISP2), pale brown (Suter medium), pale pinkish (ISP3) to grey (ISP5, ISP6, ISP7). Greyish white aerial mycelium was well developed on ISP1, ISP2, ISP3 and ISP4, only very poor white aerial mycelium was developed at the colony margin on Suter medium with and without tyrosine, and no aerial mycelium occurred on ISP5, ISP6 or ISP7 (Figs S1–S3). Straight chains of two, three and rarely four cylindrical spores with a smooth shape are formed on the tip of sporulating aerial mycelium on ISP2 (Fig. 3a, c). In contrast, the closest relative *A. rayongensis* DSM 102126^T exhibited green substrate mycelium on ISP6, light ochre substrate mycelium on ISP7 and brown substrate mycelium without aerial mycelium on Suter medium. One of the main physiological differences between RB29^T and *A. rayongensis* DSM 102126^T is the different temperature tolerance and a pronounced red pigment production in RB29^T caused by the production of rubterolones [30, 50] (Figs S1–S3 and S7, Table S6). These findings were supported by additional comparative genome analyses and MS analysis showing that *A. rayongensis* DSM 102126^T neither produces typical representatives of the rubterolone family nor harbours homologues of the responsible *rbl* genes (Fig. S7).

In summary, strain RB29^T exhibited only a few distinct different phenotypic and growth characteristics compared to the closest reference type strain *A. ayongensis* DSM 102126^T, but several distinct phenotypic characteristics compared to *A. atramentaria* DSM 43919^T (Table S6).

For strain RB68^T, phenotypic and growth characteristics can be described as follows. It was capable of growing on all media tested, tolerated a pH range of 6–8 (optimal pH 7.0) and NaCl concentration of 0–4% (w/v) (optimal 0–1%, Table 1). Strain RB68^T exhibited well-developed substrate mycelium on all media of grey to greenish (ISP1, ISP2 and ISP6), white (ISP3 and ISP4), beige (ISP5) or bright ochre (ISP7) and light brown (Suter medium) colour (Table S6, Figs S4–S6). Sparse aerial mycelium was developed on ISP2, ISP3 and ISP4 media. A brown pigment was observed on Suter medium (supplemented with tyrosine). Straight chains of two to five cylindrical warty spores were formed on the aerial mycelium (Fig. 3b, d). Overall, strain RB68^T exhibited several different phenotypic characteristics from the reference type strain *A. hibisca* DSM 44148^T (Tables 1 and S5), which clearly supported its status as representing a novel bacterial species.

PROTOLOGUE

Description of *Actinomadura rubteroloni* sp. nov.

Actinomadura rubteroloni (rub.ter.o.lo´ni. N.L. neut. n. *rubterolonum* rubterolone; N.L. gen. n. *rubteroloni* of rubterolone).

Aerobic, Gram-positive actinobacterium forming a branched vegetative mycelium. Good growth occurs on ISP1, ISP2, ISP3, ISP5, ISP6, ISP7 and Suter medium and moderate growth occurs on ISP4. Aerial mycelium is formed on all media within 6 days except ISP5, ISP6 and ISP7. Straight chains of two, three and rarely four cylindrical spores of smooth shape are formed on the tip of sporulating aerial mycelium on ISP2 agar. Red to pinkish pigments (identified as rubterolones) are produced on ISP1, ISP2, ISP3, ISP4, ISP5, ISP6 and Suter medium and a brown pigment on ISP7. The pH range for growth is 5–7. The maximum concentration of NaCl for growth is 4% (w/v) supplemented on ISP2. Growth occurs at 20–37 °C on ISP2 agar. Can grow with glucose as sole carbon source, but not with D-arabinose, D-xylose, D-mannitol, raffinose, cellulose, sucrose, inositol, D-fructose or L-rhamnose. The cell-wall peptidoglycan contains *meso*-A_2pm. The sugars in whole-cell hydrolysates are galactose, glucose, and trace madurose, mannose and ribose. The major polar lipids are diphosphatidylglycerol, phosphatidylglycerol, phosphatidylinositol and phosphatidylinositol mannoside. The predominant menaquinones are MK-9(H_6) and MK-9(H_8). The major fatty acids are 10-methyloctadecanoic acid (10-methyl $C_{18:0}$), 14-methylpentadecanoic acid (iso-$C_{16:0}$), 10-methylheptadecanoic acid (10-methyl $C_{17:0}$), hexadecanoic acid ($C_{16:0}$) and *cis*-9-octadecanoic acid ($C_{18:1}$ ω9*c*).

The type strain is RB29^T (=CCUG 72668^T=NRRL B-65537^T), which was isolated from the gut of the termite *Macrotermes natalensis* (major worker). The DNA G+C content of the type strain is 73.1 mol%. The GenBank/EMBL accession number for the partial 16S rRNA gene sequence of strain RB29^T (alias 5-2) is KY312019.2. The whole genome shotgun (WGS) project has project accession NZ_MTBP00000000. Raw sequencing data have been deposited under accession number SRR11565158.

DESCRIPTION OF *ACTINOMADURA MACROTERMITIS* SP. NOV.

Actinomadura macrotermitis (ma.cro.ter´mi.tis. N.L. gen. n. *macrotermitis* of *Macrotermes*, of the termite genus *Macrotermes*).

Aerobic, Gram-positive actinobacterium forming branched vegetative mycelium. Good growth occurs on ISP1, ISP2, ISP5, ISP6 and ISP7 and moderate growth occurs on ISP3, ISP4 and Suter medium. Aerial mycelium is sparsely formed on ISP2, ISP3 and ISP4. Straight chains of two to five cylindrical warty spores are formed on aerial mycelium on ISP2, ISP3 and ISP4. An ochre pigment is produced on ISP5, a bright-ochre pigment on ISP7 and a brown pigment on Suter medium (supplemented with tyrosine). Growth occurs at 15–37 °C on ISP2 agar. The pH range for growth is 6–8. The maximum concentration of NaCl for growth is 4% (w/v) supplemented on ISP2. Can grow with glucose, inositol or D-fructose as sole carbon source, weak growth occurs on inositol or D-fructose as sole carbon source, but not with D-arabinose, D-xylose, D-mannitol, raffinose, cellulose, sucrose or L-rhamnose. The cell-wall peptidoglycan contains *meso*-A_2pm. The sugars in whole-cell hydrolysates are galactose, glucose, mannose, and trace madurose and ribose. The major polar lipids are diphosphatidylglycerol, phosphatidylglycerol, phosphatidylinositol and phosphatidylinositol mannoside. The predominant menaquinones are MK-9(H_4) and MK-9(H_6). The major fatty acids are hexadecanoic acid ($C_{16:0}$), *cis*-9-octadecanoic acid ($C_{18:1}\omega9c$), 10- methyloctadecanoic acid (10-methyl $C_{18:0}$), *cis*-9-hexadecanoic acid ($C_{16:1}$ $\omega9c$) and 14-methylpentadecanoic acid (iso-$C_{16:0}$).

The type strain is RB68^T (=CCUG 72669^T=NRRL B-65538^T), which was isolated from the gut of the termite *Macrotermes natalensis* (major worker). The DNA G+C content of the type strain is 73.1 mol%. The GenBank/EMBL accession number for the partial 16S rRNA gene sequence of strain RB68^T is MH044510.2. The whole genome shotgun (WGS) project has project accession NZ_WEGH00000000. The raw sequencing data have been deposited under accession number SRR11566452.

Funding information
R.B. is supported by the International Leibniz Research School for Microbial and Biomolecular Interactions (ILRS) and Jena School for Microbial Communication (JSMC, DFG). The financial support of the Boehringer Ingelheim Foundation, the Daimler Benz foundation and the German research Foundation (CRC 1127, ChemBioSys and BE-4799/3-1) to C.B. is greatly acknowledged.

Acknowledgements
We thank the Oerlemans family (Mookgophong) for permission to sample colonies at their farm, and Susanne Linde (Elektronenmikroskopisches Zentrum FSU Jena) for electron micrographs.

Conflicts of interest
The authors declare that there are no conflicts of interest.

References

1. Lechevalier MP, De Bievre C, Lechevalier H. Chemotaxonomy of aerobic actinomycetes: phospholipid composition. *Biochem Syst Ecol* 1977;5:249–260.
2. Kroppenstedt RM, Goodfellow M. The family *Thermomonosporaceae: Actinocorallia, Actinomadura, Spirillospora* and *Thermomonospora*. In: Dworkin M, Falkow S, Rosenberg E, Schleifer KH, Stackebrandt E (editors). *The Prokaryotes*. USA: Springer-Verlag; 2006. pp. 682–724.
3. Zhang Z, Kudo T, Nakajima Y, Wang Y. Clarification of the relationship between the members of the family *Thermomonosporaceae* on the basis of 16S rDNA, 16S-23S rRNA internal transcribed spacer and 23S rDNA sequences and chemotaxonomic analyses. *Int J Syst Evol Microbiol* 2001;51:373–383.
4. Tamura T, Ishida Y, Nozawa Y, Otoguro M, Suzuki K-ichiro. Transfer of *Actinomadura spadix* Nonomura and Ohara 1971 to *Actinoallomurus spadix* gen. nov., comb. nov., and description of *Actinoallomurus amamiensis* sp. nov., *Actinoallomurus caesius* sp. nov., *Actinoallomurus coprocola* sp. nov., *Actinoallomurus fulvus* sp. nov., *Actinoallomurus iriomotensis* sp. nov., *Actinoallomurus luridus* sp. nov., *Actinoallomurus purpureus* sp. nov. and *Actinoallomurus yoronensis* sp. nov. *Int J Syst Evol Microbiol* 2009;59:1867–1874.
5. Zucchi TD, Kim B-Y, Bonda ANV, Goodfellow M. *Actinomadura xylanilytica* sp. nov., an actinomycete isolated from soil. *Int J Syst Evol Microbiol* 2013;63:576–580.
6. Songsumanus A, Kudo T, Ohkuma M, Phongsopitanun W, Tanasupawat S. *Actinomadura montaniterrae* sp. nov., isolated from mountain soil. *Int J Syst Evol Microbiol* 2016;66:3310–3316.
7. Miyadoh S, Amano S, Tohyama H, Shomura T. *Actinomadura atramentaria*, a new species of the *Actinomycetales*. *Int J Syst Bacteriol* 1987;37:342–346.
8. Wink J, Kroppenstedt RM, Seibert G, Stackebrandt E. *Actinomadura namibiensis* sp. nov. *Int J Syst Evol Microbiol* 2003;53:721–724.
9. He J, Xu Y, Sahu MK, Tian X-P, Nie G-X *et al*. *Actinomadura sediminis* sp. nov., a marine actinomycete isolated from mangrove sediment. *Int J Syst Evol Microbiol* 2012;62:1110–1116.
10. Qin S, Zhao G-Z, Li J, Zhu W-Y, Xu L-H *et al*. *Actinomadura flavalba* sp. nov., an endophytic actinomycete isolated from leaves of *Maytenus austroyunnanensis*. *Int J Syst Evol Microbiol* 2009;59:2453–2457.
11. Rachniyom H, Matsumoto A, Indananda C, Duangmal K, Takahashi Y *et al*. *Actinomadura syzygii* sp. nov., an endophytic actinomycete isolated from the roots of a jambolan plum tree (*Syzygium cumini* L. Skeels). *Int J Syst Evol Microbiol* 2015;65:1946–1949.
12. Promnuan Y, Kudo T, Ohkuma M, Chantawannakul P. *Actinomadura apis* sp. nov., isolated from a honey bee (Apis mellifera) hive, and the reclassification of *Actinomadura cremea* subsp. *rifamycini* Gauze *et al.* 1987 as *Actinomadura rifamycini* (Gauze *et al.* 1987) sp. nov., comb. nov. *Int J Syst Evol Microbiol* 2011;61:2271–2277.
13. Nakamura G, Isono K. A new species of *Actinomadura* producing a polyether antibiotic, cationomycin. *J Antibiot* 1983;36:1468–1472.
14. Oki T, Konishi M, Tomatsu K, Tomita K, Saitoh K *et al*. Pradimicin, a novel class of potent antifungal antibiotics. *J Antibiot* 1988;41:1701–1704.
15. Igarashi Y, Iida T, Oku N, Watanabe H, Furihata K *et al*. Nomimicin, a new spirotetronate-class polyketide from an actinomycete of the genus *Actinomadura*. *J Antibiot* 2012;65:355–359.
16. Kornsakulkarn J, Saepua S, Boonruangprapa T, Suphothina S, Thongpanchang C. New β-carboline and indole alkaloids from actinomycete *Actinomadura* sp. bcc 24717. *Phytochem Lett* 2013;6:491–494.
17. Benndorf R, Guo H, Sommerwerk E, Weigel C, Garcia-Altares M *et al*. Natural products from actinobacteria associated with fungus-growing termites. *Antibiotics* 2018;7:E83
18. Visser AA, Nobre T, Currie CR, Aanen DK, Poulsen M. Exploring the potential for actinobacteria as defensive symbionts in fungus-growing termites. *Microb Ecol* 2012;63:975–985.
19. Hsu SC, Lockwood JL. Powdered chitin agar as a selective medium for enumeration of actinomycetes in water and soil. *Appl Microbiol* 1975;29:422–426
20. Shirling EB, Gottlieb D. Methods for characterization of *Streptomyces* species. *Int J Syst Bacteriol* 1966;16:313–340.

21. Rutherford K, Parkhill J, Crook J, Horsnell T, Rice P *et al*. Artemis: sequence visualization and annotation. *Bioinformatics* 2000;16:944–945.
22. Parte AC. LPSN--list of prokaryotic names with standing in nomenclature. *Nucleic Acids Res* 2014;42:D613–D616.
23. Meier-Kolthoff JP, Göker M, Spröer C, Klenk H-P. When should a DDH experiment be mandatory in microbial taxonomy? *Arch Microbiol* 2013b;195:413–418.
24. Pruesse E, Peplies J, Glöckner FO. SINA: accurate high-throughput multiple sequence alignment of ribosomal RNA genes. *Bioinformatics* 2012;28:1823–1829.
25. Saitou N, Nei M. The neighbor-joining method: a new method for reconstructing phylogenetic trees. *Mol Biol Evol* 1987;4:406–425.
26. Felsenstein J. Evolutionary trees from DNA sequences: a maximum likelihood approach. *J Mol Evol* 1981;17:368–376.
27. Kumar S, Stecher G, Tamura K. MEGA7: molecular evolutionary genetics analysis version 7.0 for bigger datasets. *Mol Biol Evol* 2016;33:1870–1874.
28. Tamura K, Nei M. Estimation of the number of nucleotide substitutions in the control region of mitochondrial DNA in humans and chimpanzees. *Mol Biol Evol* 1993;10:512–526.
29. Felsenstein J. Confidence limits on phylogenies: an approach using the bootstrap. *Evolution* 1985;39:783–791.
30. Guo H, Benndorf R, Leichnitz D, Klassen JL, Vollmers J *et al*. Isolation, biosynthesis and chemical modifications of Rubterolones A-F: rare tropolone alkaloids from *Actinomadura* sp. 5-2. *Chem Eur J* 2017;23:9338–9345.
31. Auch AF, Klenk H-P, Göker M. Standard operating procedure for calculating genome-to-genome distances based on high-scoring segment pairs. *Stand Genomic Sci* 2010;2:142–148.
32. Meier-Kolthoff JP, Auch AF, Klenk H-P, Göker M. Genome sequence-based species delimitation with confidence intervals and improved distance functions. *BMC Bioinformatics* 2013;14:60.
33. Meier-Kolthoff JP, Klenk H-P, Göker M. Taxonomic use of DNA G+C content and DNA-DNA hybridization in the genomic age. *Int J Syst Evol Microbiol* 2014;64:352–356.
34. Goris J, Konstantinidis KT, Klappenbach JA, Coenye T, Vandamme P *et al*. DNA-DNA hybridization values and their relationship to whole-genome sequence similarities. *Int J Syst Evol Microbiol* 2007;57:81–91.
35. Richter M, Rosselló-Móra R, Oliver Glöckner F, Peplies J. JSpeciesWS: a web server for prokaryotic species circumscription based on pairwise genome comparison. *Bioinformatics* 2016;32:929–931.
36. Yoon S-H, Ha S-M, Lim J, Kwon S, Chun J. A large-scale evaluation of algorithms to calculate average nucleotide identity. *Antonie van Leeuwenhoek* 2017;110:1281–1286.
37. Meier-Kolthoff JP, Göker M. TYGS is an automated high-throughput platform for state-of-the-art genome-based taxonomy. *Nat Commun* 2019;10:2182.
38. Chun J, Oren A, Ventosa A, Christensen H, Arahal DR *et al*. Proposed minimal standards for the use of genome data for the taxonomy of prokaryotes. *Int J Syst Evol Microbiol* 2018;68:461–466.
39. Hasegawa T, Takizawa M, Tanida S. A rapid analysis for chemical grouping of aerobic actinomycetes. *J Gen Appl Microbiol* 1983;29:319–322.
40. Schumann P. Peptidoglycan structure. In: Rainey F, Oren A (editors). *Taxonomy of Prokaryotes, Methods in Microbiology*, 38. London: Academic Press. pp. 101–129.
41. Minnikin DE, Alshamaony L, Goodfellow M. Differentiation of Mycobacterium, *Nocardia*, and related taxa by thin-layer chromatographic analysis of whole-organism methanolysates. *J Gen Microbiol* 1975;88:200–204.
42. Collins MD, Pirouz T, Goodfellow M, Minnikin DE. Distribution of menaquinones in actinomycetes and corynebacteria. *J Gen Microbiol* 1977;100:221–230.
43. Wink J, Schumann P, Atasayar E, Klenk H-P, Zaburannyi N *et al*. '*Streptomyces caelicus*', an antibiotic-producing species of the genus *Streptomyces*, and *Streptomyces canchipurensis* Li *et al.* 2015 are later heterotypic synonyms of *Streptomyces muensis* Ningthoujam *et al.* 2014. *Int J Syst Evol Microbiol* 2017;67:548–556.
44. Minnikin DE, Collins MD, Goodfellow M. Fatty acid and polar lipid composition in the classification of *Cellulomonas*, *Oerskovia* and related taxa. *J Appl Bacteriol* 1979;47:87–95.
45. Collins MD, Jones D. Lipids in the classification and identification of coryneform bacteria containing peptidoglycans based on 2, 4-diaminobutyric acid. *J Appl Bacteriol* 1980;48:459–470.
46. Leibniz Institute DSMZ. German Collection of Microorganisms and Cell Cultures GmbH. Available from: https://www.dsmz.de/services/services-microorganisms/identification/analysis-of-cellular-fatty-acids.html.
47. Groth I, Schumann P, Rajney FA, Martin K, Schuetze B *et al*. *Bogoriella caseilytica* gen. nov., sp. nov., a new alkaliphilic actinomycete from a soda lake in Africa. *Int J Syst Bacteriol* 1997;47:788–794.
48. Suter MA. Isolierung und Charakterisierung von Melanin-negativen Mutanten aus *Streptomyces glaucescens*. *ETH Zürich Doktorarbeit* 1978.
49. Xu P, Li W-J, Tang S-K, Zhang Y-Q, Chen G-Z *et al*. *Naxibacter alkalitolerans* gen. nov., sp. nov., a novel member of the family '*Oxalobacteraceae*' isolated from China. *Int J Syst Evol Microbiol* 2005;55:1149–1153.
50. Guo H, Benndorf R, König S, Leichnitz D, Weigel C *et al*. Expanding the Rubterolone family: intrinsic reactivity and directed diversification of PKS-derived pyrans. *Chem Eur J* 2018;24:11319–11324.